AD-A121 857 DIELECTRIC WAVEGUIDE GRATING FILTER(U) ILLINOIS UNIV AT URBANA ELECTROMAGNETICS LAB K WEBB ET AL. NOV 82 UIEM-82-11 ARO-18054.4-EL DAAG29-82-K-0084 1/1

UNCLASSIFIED F/G 9/5 NL

END

FILMED

DTIC

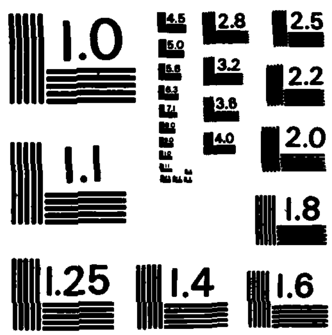

MICROCOPY RESOLUTION TEST CHART
NATIONAL BUREAU OF STANDARDS-1963-A

ELECTROMAGNETICS LABORATORY
INTERIM TECHNICAL REPORT NO. 82-11

November 1982

DIELECTRIC WAVEGUIDE GRATING FILTER

K. WEBB

R. MITTRA

ELECTROMAGNETICS LABORATORY
DEPARTMENT OF ELECTRICAL ENGINEERING
ENGINEERING EXPERIMENT STATION
UNIVERSITY OF ILLINOIS AT URBANA-CHAMPAIGN
URBANA, ILLINOIS 61801

SUPPORTED BY
U.S. ARMY RESEARCH OFFICE
GRANT NO. DAAG29-82-K-0084
JOINT SERVICES ELECTRONICS PROGRAM
N00014-79-C-0424

UNCLASSIFIED

SECURITY CLASSIFICATION OF THIS PAGE (When Data Entered)

REPORT DOCUMENTATION PAGE

READ INSTRUCTIONS BEFORE COMPLETING FORM

1. REPORT NUMBER

2. GOVT ACCESSION NO. A121857

3. RECIPIENT'S CATALOG NUMBER

4. TITLE (and Subtitle)
DIELECTRIC WAVEGUIDE GRATING FILTER

5. TYPE OF REPORT & PERIOD COVERED
Interim Technical

6. PERFORMING ORG. REPORT NUMBER
EM 82-11; UILU-ENG-82-2551

7. AUTHOR(s)
K. Webb and R. Mittra

8. CONTRACT OR GRANT NUMBER(s)
DAAG29-82-K-0084
(N00014-79-C-0424)
(Joint Services Elec. Program)

9. PERFORMING ORGANIZATION NAME AND ADDRESS
Electromagnetics Laboratory
Department of Electricl Engineering
University of Illinois, Urbana, Illinois 61801

10. PROGRAM ELEMENT, PROJECT, TASK AREA & WORK UNIT NUMBERS

11. CONTROLLING OFFICE NAME AND ADDRESS
U. S. Army Research Office
P. O. Box 12211
Research Triangle Park, NC 27709

12. REPORT DATE
November 1982

13. NUMBER OF PAGES
20

14. MONITORING AGENCY NAME & ADDRESS (if different from Controlling Office)

15. SECURITY CLASS. (of this report)
UNCLASSIFIED

15a. DECLASSIFICATION/DOWNGRADING SCHEDULE

16. DISTRIBUTION STATEMENT (of this Report)
APPROVED FOR PUBLIC RELEASE;
DISTRIBUTION UNLIMITED

17. DISTRIBUTION STATEMENT (of the abstract entered in Block 20, if different from Report)

18. SUPPLEMENTARY NOTES
The view, opinions, and/or findings contained in this report are those of the author(s) and should not be construed as an official Department of the Army position, policy, or decision, unless so designated by other documentation.

19. KEY WORDS (Continue on reverse side if necessary and identify by block number)
millimeter waves and quasi-optics; grating filters; dielectric waveguide

20. ABSTRACT (Continue on reverse side if necessary and identify by block number)
A dielectric waveguide grating structure may be used as a band-reject filter. A transmission line model is used to predict the filter response. The experimental results agree well with theoretical predictions.

DD FORM 1 JAN 73 1473 EDITION OF 1 NOV 65 IS OBSOLETE

UNCLASSIFIED

SECURITY CLASSIFICATION OF THIS PAGE (When Data Entered)

UILU-ENG-82-2551

Electromagnetics Laboratory Report No. 82-11

DIELECTRIC WAVEGUIDE GRATING FILTER

by

K. Webb
R. Mittra

Electromagnetics Laboratory
Department of Electrical Engineering
University of Illinois at Urbana-Champaign
Urbana, Illinois 61801

Interim Technical Report

November 1982

Supported by

U. S. Army Research Office
Grant No. DAAG29-82-K-0084
Joint Services Electronics Program
N00014-79-C-0424

TABLE OF CONTENTS

LIST OF FIGURES

I. INTRODUCTION

Dielectric waveguide (DWG) filter structures are of particular interest for millimeter-wave and optical applications. A number of applications have been reported recently in the millimeter wave and quasi-optical areas [1]-[3] and optical grating filters have been reported in [4]. Grating-type dielectric waveguide filters have several advantages over alternative configurations, such as the ring-resonator filter [5], [6]. In particular, the ring-resonator should be a number of wavelengths in circumference for satisfactory performance, which implies closely spaced spurious pass- or stop-bands. The grating filter can easily be incorporated in an integrated system, and may be realized by a series of discontinuities, such as surface or dielectric variations.

There has been some work done on complex mode-matching methods [7] in an effort to analyze discontinuities in dielectric waveguide. It is somewhat impractical to apply these techniques to grating filter response analysis. It is proposed in this paper that a simple transmission line model may be used to analyze such a grating structure. Experimentation has verified this approach. The theory developed is valid for any form of dielectric waveguide.

Section II gives details of the theoretical analysis of the dielectric waveguide grating filter. Experimental results are given in Section III. Conclusions are outlined in Section IV.

II. ANALYSIS OF DIELECTRIC WAVEGUIDE GRATING STRUCTURE

A stepped dielectric grating structure and transmission line model are shown in Fig. 1. Image Guide (rectangular dielectric guide on a ground plane) will be considered specifically, although the approach may be

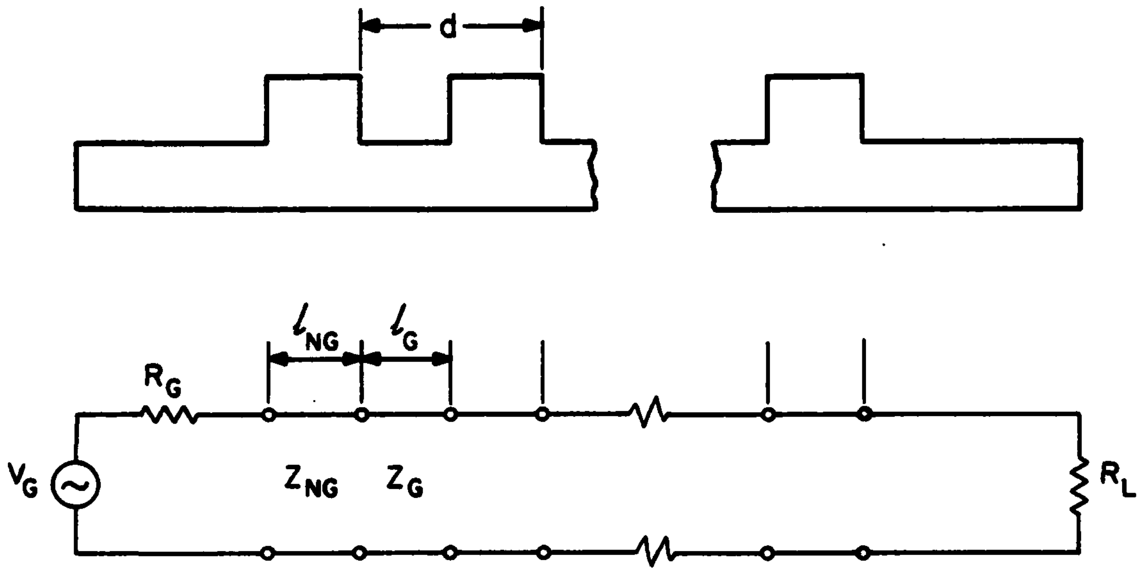

Figure 1. Image guide grating filter and transmission line model.

generalized to other dielectric waveguides. It is proposed that this model may be used for an approximate analysis of the grating filter.

The dielectric waveguide supports hybrid modes, which may be expressed as a sum of transverse electric and transverse magnetic modes, or longitudinal section electric (LSE) and magnetic (LSM) modes. The LSE fields may be expressed as [8]

$$\bar{E} = -j\omega\mu\nabla \times \Pi_h \tag{1a}$$

$$\bar{H} = \varepsilon_r k_0^2 \Pi_h + \nabla\nabla\cdot\Pi_h \tag{1b}$$

and the LSM fields as

$$\bar{E} = k_0^2 \Pi_e + \nabla(\varepsilon_r^{-1}\nabla\cdot\Pi_e) \tag{2a}$$

$$\bar{H} = j\omega\varepsilon_0 \nabla \times \Pi_e \tag{2b}$$

where Π_h and Π_e are the magnetic and electric Hertzian potentials, respectively.

With $\Pi_h = \hat{y}\ \phi_h(x,y)e^{-j\beta z} = \hat{y}\ \phi_h$ and $\Pi_e = \hat{y}\ \phi_e$ the dielectric waveguide fields may be expressed in terms of electric and magnetic scalar potential functions.

$$E_x = \frac{1}{\varepsilon_r(y)} \frac{\partial^2 \phi_e}{\partial x \partial y} + \omega\mu_0\beta\phi_h$$

$$E_y = \frac{1}{\varepsilon_r(y)} \left(\beta^2\phi_e - \frac{\partial^2\phi_e}{\partial x^2}\right)$$

$$E_z = -j\omega\mu_0 \frac{\partial\phi_h}{\partial x} - \frac{j\beta}{\varepsilon_r(y)} \frac{\partial\phi_e}{\partial y}$$

$$H_x = \frac{\partial^2\phi_h}{\partial x \partial y} - \omega\varepsilon_0\beta\phi_e$$

$$H_y = \beta^2 \phi_h - \frac{\partial^2 \phi_h}{\partial x^2}$$

$$H_z = -j\beta \frac{\partial \phi_h}{\partial y} + j\omega\varepsilon_0 \frac{\partial \phi_e}{\partial x} \tag{3}$$

The effective dielectric constant method [9], [10] is a very suitable approach for finding the propagation constant in planar dielectric waveguides. Various forms of dielectric waveguide may be analyzed in this manner. Consider the image guide structure of Fig. 2. Using the effective dielectric constant method and matching the fields in each region the following eigenvalue equations may be found. The equation for k_y is

$$\varepsilon_r \sqrt{k_0^2(\varepsilon_r - 1) - k_y^2} \cos k_y y_1 - k_y \sin k_y y_1 = 0 \tag{4}$$

where ε_r is the relative permittivity of the guide. After solving for k_y, the effective dielectric constant (ε_{e2}) for region 2 may be found.

$$\varepsilon_{e2} = \varepsilon_r - \frac{k_y^2}{k_0^2} \tag{5}$$

The equation for k_x is

$$\left[k_0^2(\varepsilon_{e2} - 1) - 2k_x^2\right] \sin k_x(x_2 - x_1) + 2k_x \sqrt{k_0^2(\varepsilon_{e2} - 1) - k_x^2} \cos k_x(x_2 - x_1) \tag{6}$$

Thus the guide propagation constant becomes

$$\beta = \sqrt{\varepsilon_{e2} k_0^2 - k_x^2} \tag{7}$$

The dominant mode is considered in this paper. We will define the waveguide characteristic impedance

$$Z = \eta_0 \frac{k_0}{\beta} \tag{8}$$

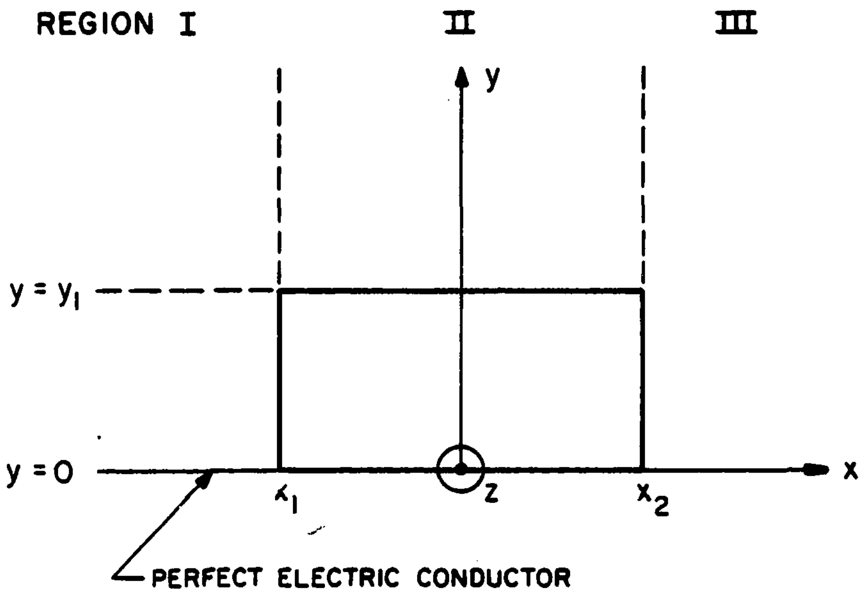

Figure 2. Image guide with coordinate system.

where η_0, k_0 are the free-space wave impedance and propagation constant respectively.

In order to find the filter transfer-function, consider the unit cell shown in Fig. 3. The ABCD matrix for the unit cell may be obtained by multiplying the matrices for two line sections [11]. The unit cell matrix is

$$\begin{bmatrix} A & B \\ C & D \end{bmatrix}_1$$

$$A = \cos(\beta_G \ell_G)\cos(\beta_{NG}\ell_{NG}) - \frac{\beta_{NG}}{\beta_G}\sin(\beta_G \ell_G)\sin(\beta_{NG}\ell_{NG})$$

$$B = j\eta_0\left[\frac{k_o}{\beta_{NG}}\cos(\beta_G \ell_G)\sin(\beta_{NG}\ell_{NG}) + \frac{k_o}{\beta_G}\sin(\beta_G \ell_G)\cos(\beta_{NG}\ell_{NG})\right]$$

$$C = j\,\frac{1}{\eta_0}\left[\frac{\beta_G}{k_0}\sin(\beta_G \ell_G)\cos(\beta_{NG}\ell_{NG}) + \frac{\beta_{NG}}{k_0}\cos(\beta_G \ell_G)\sin(\beta_{NG}\ell_{NG})\right]$$

$$D = \cos(\beta_G \ell_G)\cos(\beta_{NG}\ell_{NG}) - \frac{\beta_G}{\beta_{NG}}\sin(\beta_G \ell_G)\sin(\beta_{NG}\ell_{NG}) \qquad (9)$$

The ABCD matrix for a grating structure of n unit cells is obtained by raising the matrix for a single cell to the n^{th} power.

The transducer loss ratio is given by [10]

$$\frac{P_{avail}}{P_L} = \frac{1}{4R_G R_L}\left[(AR_L + DR_G)^2 + \left(\frac{B + CR_G R_L}{j}\right)^2\right] \qquad (10)$$

where P_L is the power delivered to R_L and $P_{avail} = |V_g|^2/4R_G$ is the available power from the generator. Thus we have a method for computing the filter insertion loss (P_L/P_{avail}) as a function of frequency. It should be noted that the effects of the discontinuities have been ignored at this stage. Although this is quite approximate the response predicted

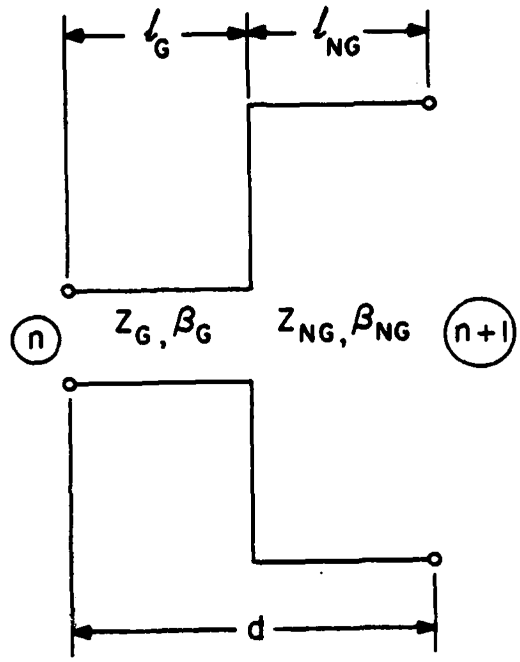

Figure 3. Unit cell in transmission-line model.

from such an analysis agrees well with measurements.

Fields in a periodic structure can be expressed in terms of spatial harmonics, according to Floquet's Theorem [12]. The propagation constants are

$$\beta_n = \beta_0 + \frac{2\pi n}{d}, \quad n = 0, \pm 1, \pm 2, \ldots \tag{11}$$

where d is the grating period. It is useful to look at the dispersion curves on a k_0d - βd diagram, such as Fig. 4. Coupled mode theory may be used to explain the filter characteristics. There is a stop-band when

$$\beta d = \Pi \tag{12}$$

where β is the propagation constant in the grating. At this frequency there is coupling between the spatial harmonics $(\beta_0)_+$ and $(\beta_{-1})_-$, which propagate in opposite directions. The waves are guided by the structure (slow wave region). The grating exhibits a reflection coefficient close to one in the stop-band, and close to zero either side.

Consider ports n and n+1 in the unit cell of Fig. 3, when the cell is part of a periodic structure.

$$\begin{bmatrix} V_n \\ I_n \end{bmatrix} = \begin{bmatrix} A & B \\ C & D \end{bmatrix} \begin{bmatrix} V_{n+1} \\ I_{n+1} \end{bmatrix} = e^{\gamma d} \begin{bmatrix} V_{n+1} \\ I_{n+1} \end{bmatrix} \tag{13}$$

For a lossless reciprocal network [13],

$$\cos \beta d = \frac{A+D}{2} \tag{14}$$

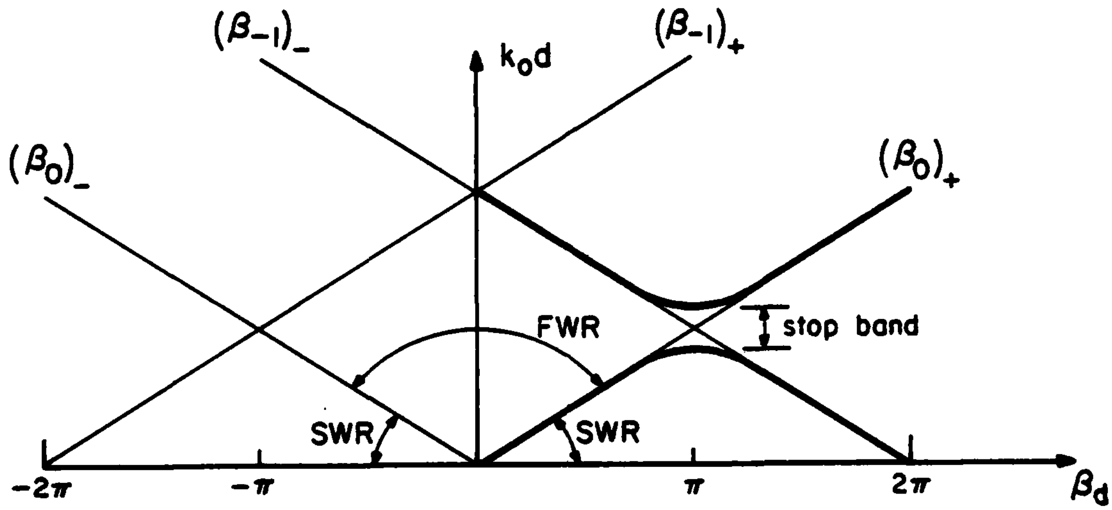

Figure 4. k_0d-βd diagram $(\beta_n)_+$ are forward travelling space harmonics and $(\beta_n)_-$ are backward travelling space harmonics.

The following relationship may thus be derived

$$\cos \beta d = \cos\beta_G \ell_G \cos \beta_{NG}(d-\ell_G) - 1/2 \left(\frac{\beta_G}{\beta_{NG}} + \frac{\beta_{NG}}{\beta_G}\right) \sin \beta_G \ell_G \sin \beta_{NG}(d-\ell_G) \quad (15)$$

For a particular d/ℓ_G, the required d may be found from (15) once the propagation constants β_G and β_{NG} for a uniform guide are found from (4)-(7).

III. RESULTS AND DISCUSSION

Filter designs and response predictions were achieved using the procedures outlined in Section II with the aid of computer programs.

A scaled image-guide filter was built and tested at X-band. The dimensions and predicted and measured insertion loss responses are shown in Fig. 5. Figure 6 shows a photograph of the filter. Rexolite 1422 was used as the dielectric, due to its favorable electrical and mechanical qualities. To enable testing with a network analyzer system, a suitable transition between metal waveguide and DWG is necessary. The transition used consists of a horn and a H-plane tapered section of DWG. This has been shown to act as a low-loss transition.

The predicted response is for matched loads at midband. (Maximum ripple across band due to mismatch is less than 1 dB). Equation (14) predicts the lower edge of the stop-band, so a slight adjustment is necessary to obtain a required center frequency. The measurements agree well with predictions. In particular, it should be noted that the location and width of the stop-band and the lower frequency ripple are accurately predicted. Measured data in the 11-12 GHz range deviated from the predicted

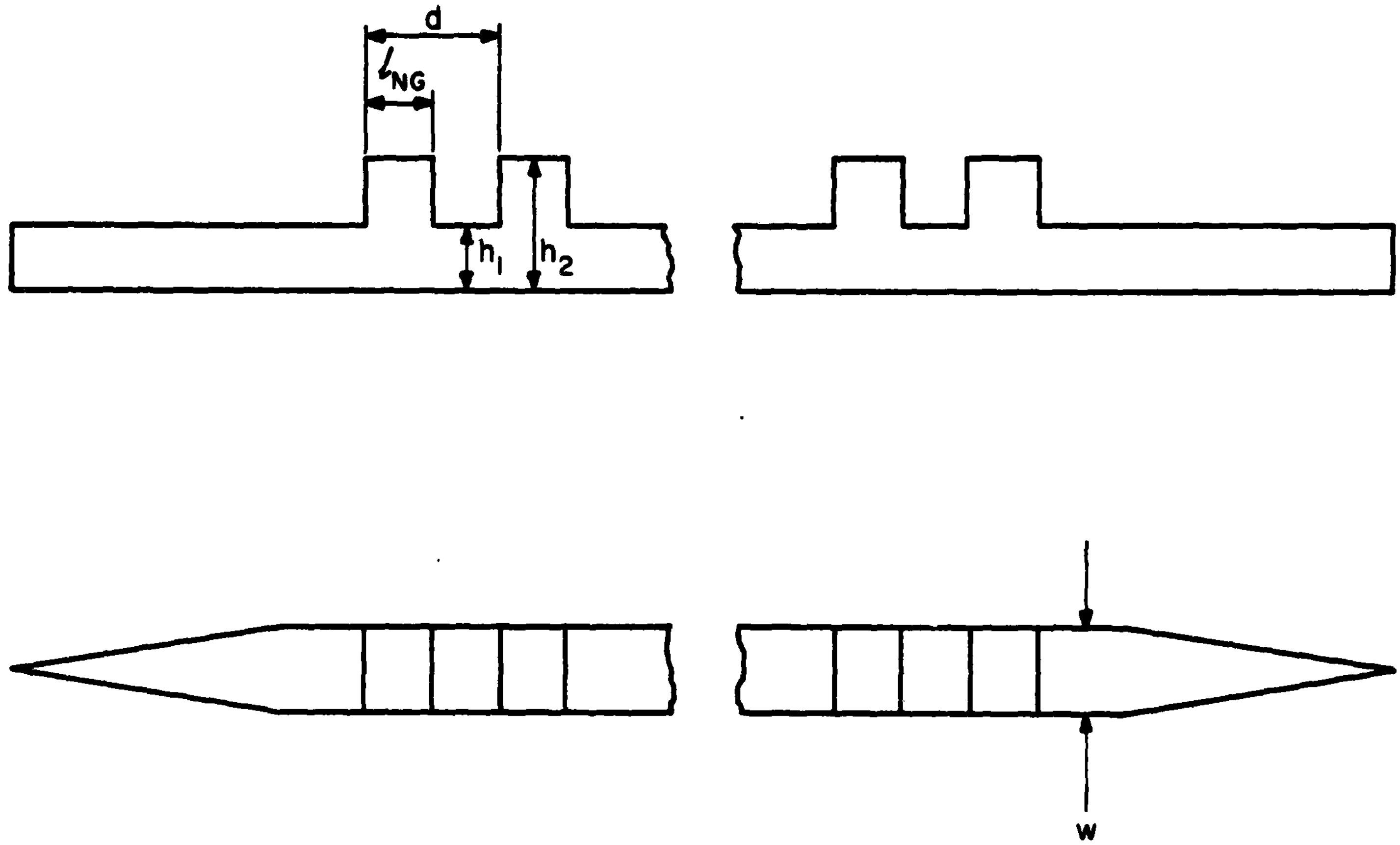

Figure 5a. Grating filter tested. N = 20 sections (unit cells), ℓ_{NG}/d = 0.5, d = 11.2 mm, h_1 = 7 mm, h_2 = 17 and 20 mm, w = 20 mm, ε_r = 2.53 Rexolite 1422.

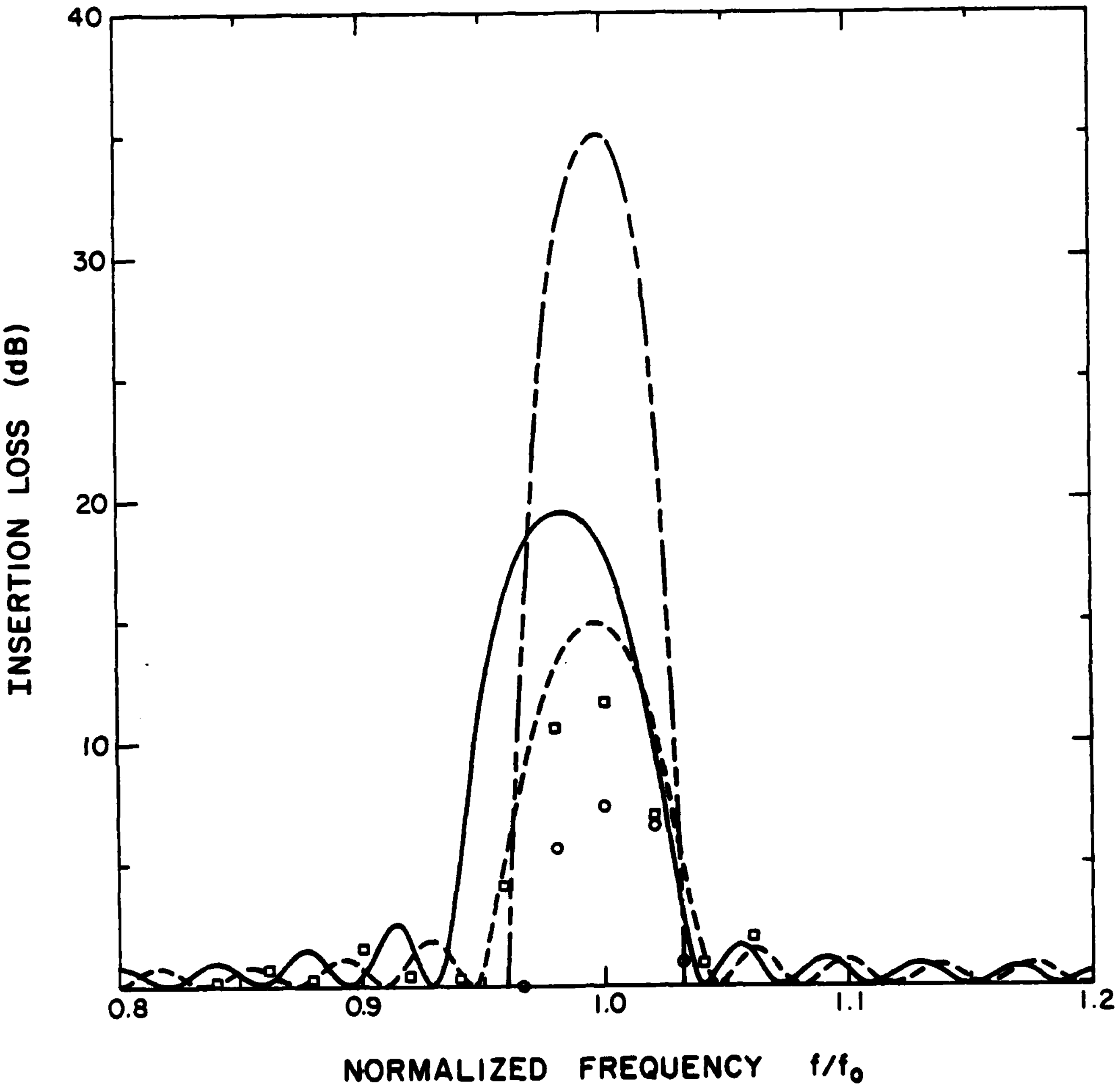

Figure 5b. Predicted and measured insertion losses for grating filter.

h_1 = 7 mm, ℓ_{NG}/d = 0.5, d = 11.2 mm, f_0 = 10 GHz.

Predicted: ——————— h_2 = 20 mm } N = 20 sections

– – – – – – – h_2 = 14 mm }

——— – – ——— h_2 = 14 mm N = 40 sections

Measured: □ h_2 = 20 mm; ○ h_2 = 14 mm N = 20 sections.

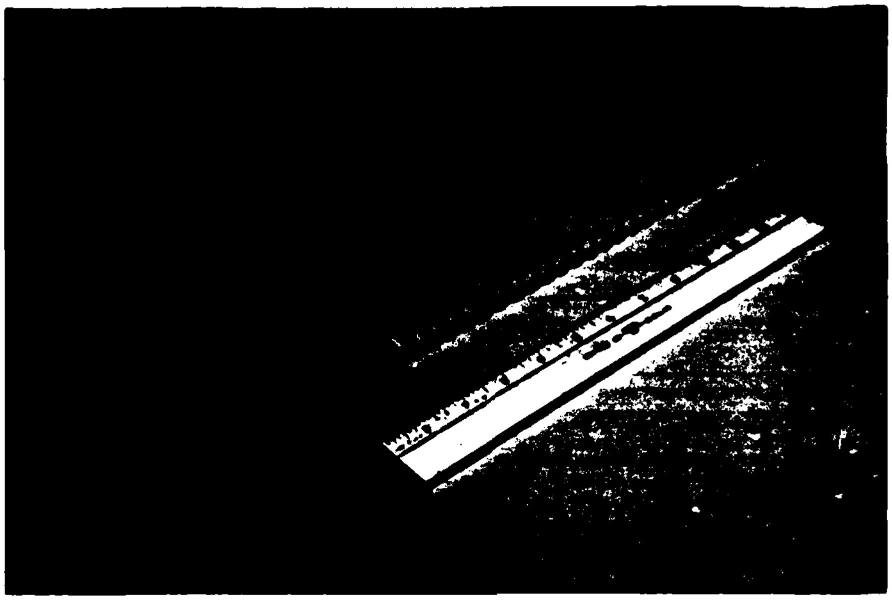

Figure 6. Image guide grating filter.

response. This deviation was due to radiation in this frequency range. It is generally accepted that grating-type slow-wave DWG structures have some inherent radiation problems. However, the radiation region may not cause a problem and could possibly be eliminated by matching. Matching of the periodic structure may be achieved via tapered steps at the ends [13].

Increasing the number of sections or the step size increases the stop-band insertion loss. A large step results in a slightly larger stop-bandwidth, and increasing the number of sections narrows the stop-bandwidth. ℓ_{NG}/d values other than 0.5 reduce the stop-bandwidth and decrease the stop-band insertion loss, especially for ℓ_{NG}/d 0.5.

There are a number of interesting filter structures which employ gratings. These include:

(i) Stagger tuned grating sections in series to realize a low-pass or large stop-band band-reject filter (Fig. 7(a)).

(ii) Grating with coupler. (Fig. 7(b)). The forward coupler action couples the reflected power from the grating to achieve a band-pass response between parts 1 and 2.

(iii) Tapering in the grating to obtain an equal-ripple response. The realizable β_G/β_{NG} limits this.

IV. CONCLUSIONS

A simple yet effective means of analyzing dielectric waveguide grating filters has been presented. Experimentation has verified the theoretical analysis. This technique thus becomes a very useful design tool which is applicable to many forms of periodic and non-periodic guided wave structures.

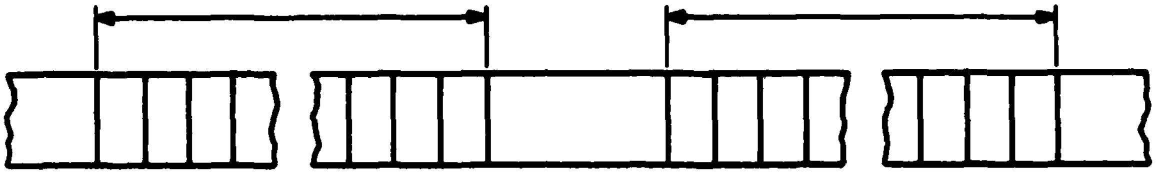

Figure 7a. Series stagger-tuned grating filter.

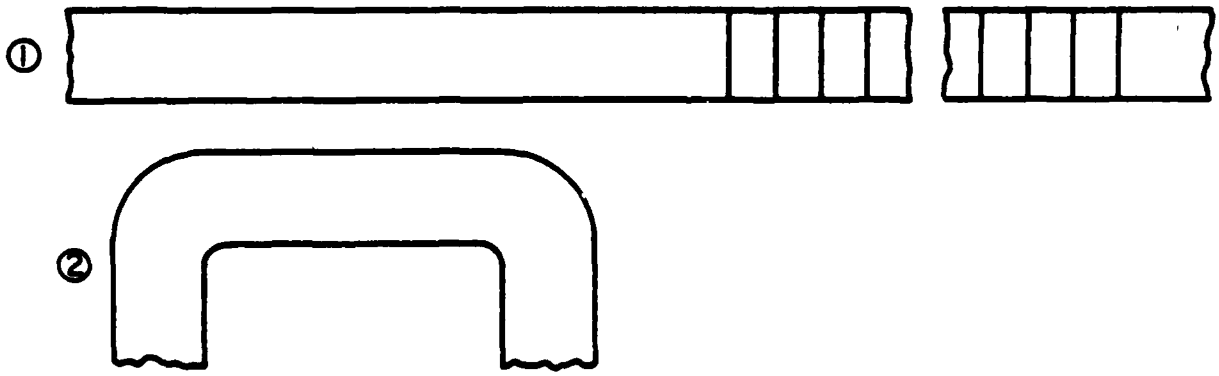

Figure 7b. Filter consisting of grating with coupler.

V. REFERENCES

1. Itoh, T. "Application of gratings in a dielectric waveguide for leaky-wave antennas and band-reject filters." IEEE Trans. Microwave Theory & Tech., vol. MTT-25, no. 12, pp. 1134-1138, Dec. 1977.
2. Song, B., Itoh, T. "Distributed Bragg reflection dielectric waveguide oscillators." IEEE Trans. Microwave Theory & Tech., vol. MTT-27, no. 12, pp. 1019-1022, Dec. 1979.
3. Itoh, T., Hsu, F. "Distributed Bragg reflector gunn oscillators for dielectric millimeter-wave integrated circuits." IEEE Trans. Microwave Theory & Tech., vol. MTT-27, no. 5, pp. 514-518, May 1979.
4. Schmidt, R. et al., "Narrow-band grating filters for thin-film optical waveguides." Appl. Phys. Letts., vol. 25, no. 11, pp. 651-652, Dec. 1974.
5. Itanami, J., Shindo, S. "Channel dropping filter for millimeter-wave integrated circuits." IEEE Trans. Microwave Theory & Tech., vol. MTT-26, no. 10, pp. 759-764, Oct. 1978.
6. Kietzer, J., Kaurs, A., Levin, B. "A V-band comm. transmitter and receiver system using dielectric waveguide integrated circuits." IEEE Trans. Microwave Theory & Tech., vol. MTT-24, no. 11, pp. 797-803, Nov. 1976.
7. Rozzi T., In't Veld G., "Field and network analysis of interacting step discontinuities in planar dielectric waveguides," IEEE Trans. Microwave Theory & Tech., vol. MTT-27, no. 4, pp. 303-309, April 1979.
8. Collin, R. "Field theory of guided waves," Chap. 6. McGraw-Hill, 1960.
9. Knox, R., Toulios, P. "Integrated circuits for the millimeter through optical frequency range." Symposium on submillimeter waves. Polytechnic Institute of Brooklyn. March 31, 1970.

10. McLevige W., Itoh, T., Mittra, R. "New waveguide structures for millimeter-wave and optical integrated circuits." IEEE Trans. Microwave Theory & Tech., vol. MTT-23, no. 10, pp. 788-794, Oct. 1975.

11. Matthaei, G., Young, L., Jones, E. "Microwave filters, impedance matching networks and coupling structures." Artech House, 1980.

12. Collin, R., Zucker, F. "Antenna theory Part 2." Chap. 19 , McGraw-Hill, 1969.

13. Collin, R. "Foundations of Microwave Engineering," Chap. 8 , McGraw-Hill, 1966.